Stability of Scroll Excitation Waves in Human Atria during Fibrillation: A Computational Study

S Kharche[1], CJ Garratt[1], AV Holden[2], H Zhang[1]

[1]School of Physics & Astronomy and School of Medicine, University of Manchester, Manchester, UK
[2]Institute of Membrane and Systems Biology, University of Leeds, Leeds, UK

Abstract

We computationally evaluated the functional roles of atrial fibrillation induced electrical remodelling (AFER) on human atrial electrical excitations at cellular, tissue and whole organ levels. Our results show that AFER produced a dramatic reduction in action potential duration, slowing down of intra-atrial conduction, decrease in tissue's temporal vulnerability, but remarkable increase in tissue's spatial vulnerability to arrythmogenesis in response to premature stimulus. It also increased stability of re-entrant waves in 2D and 3D models. With AFER, the rate of atrial excitation was much higher and re-entry degenerated into persistent spatio-temporal chaos. In conclusion, our simulations substantiate a link between AFER and persistence of AF. This study provided a mechanistic insight into the mechanisms underlying the perpetuation and maintenance of AF.

1. Introduction

Atrial fibrillation (AF) affects the aged population and accounts for about 1% of the total National Health Service expenditure [1] in the UK alone and also has a large prevalence in the USA [2]. AF is the most common sustained arrhythmia leading to thromboembolism and heart failure among other debilitating cardiac complications. AF is characterized by irregular re-entrant electrical propagations in the atria. Chronic *AF induced electrical remodeling* (AFER) of membrane ionic channels in individual atrial cells has been recently studied in two experimental studies [3, 4], and has been proposed as a major contributor underlying persistent as it shortens action potential duration (APD_{90}), reduces atrial conduction velocity (CV) leading to stability of re-entrant excitation. In addition, anatomical obstacles due to the opening holes of blood vessels (*e.g.* superior vena cava (SVC) and pulmonary veins) may provide a secondary mechanism to sustain AF.

In this paper, we studied the effects of AFER on the electrical activities in atrial cells and spatially extended atrial tissue. Dynamical behaviour of scroll waves in a 3D homogenous anatomical model were characterized. Our study has shown that AFER alone has a major effect on atrial conduction and scroll wave dynamics, which helps sustain AF. This study provides insights to understand how AF begets AF, by which paroxysmal AF transient to chronic AF due to AF-induced AFER.

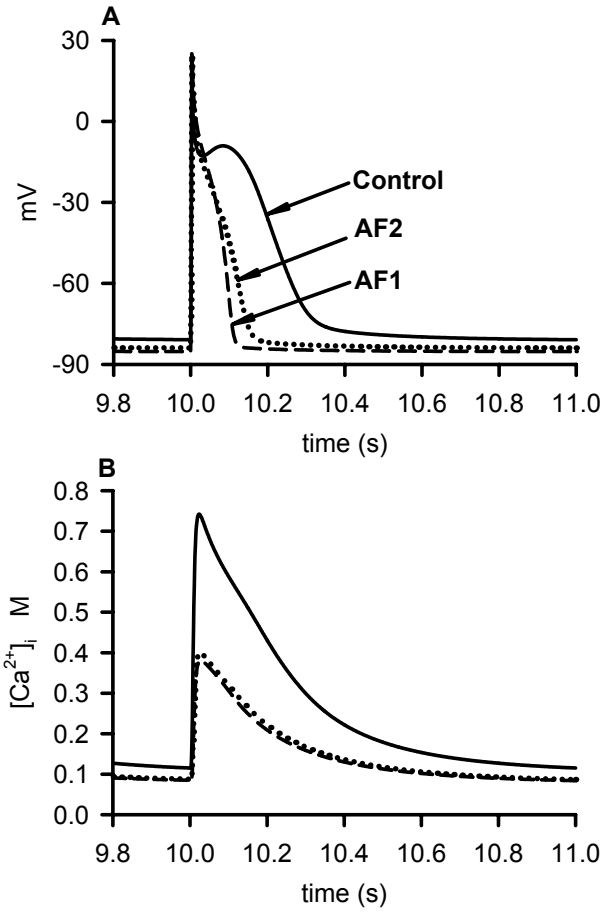

Figure 1. A. AP abbreviation produced by AFER. B. Associated changes in $[Ca^{2+}]_i$ transients. See text for details.

2. Methods

A biophysically detailed computer model for human atrial cells developed by Courtemanche *et al.* [5] was modified to incorporate experimental data of AFER on human atrial myocytes by Bosch *et al.* [3] (AF1) and Workman *et al.* [4] (AF2) to simulate AF remodeling [6]. In brief, the ionic channel remodeling in AF1 is a 235% increase in I_{K1}, 74% down regulation of $I_{Ca,L}$, 85% down regulation of I_{to}, a shift of -16 mV in the I_{to} steady-state activation, and a -1.6 mV shift of sodium current (I_{Na}) steady state activation. Fast inactivation kinetics of $I_{Ca,L}$ is slowed down, and was implemented as a 62% increase in the time constant. The ionic channel remodeling in AF2 is a 90% increase in the inward rectifier potassium current (I_{K1}), 64% down regulation of the L-type calcium current ($I_{Ca,L}$), 65% down regulation of the transient outward current (I_{to}), 12% up regulation of the sustained outward potassium current (I_{Ksus}), and a 12% down regulation of the sodium potassium pump ($I_{Na,K}$).

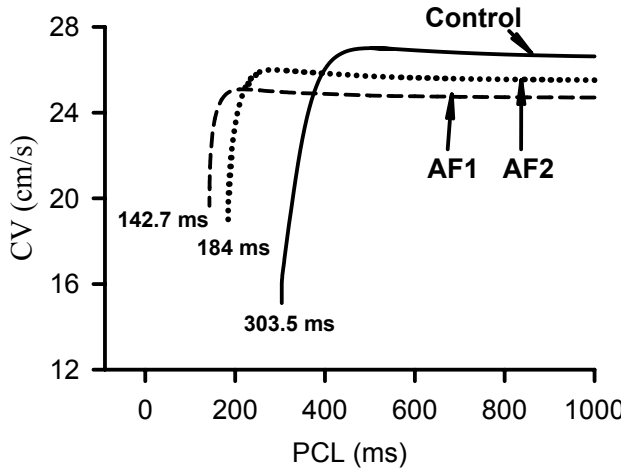

Figure 2. CVr in Control, AF1 and AF2 cases. AFER reduces solitary wave velocity, but allows propagations at much higher rates of pacing, *i.e.* smaller PCL. Propagation fails at a PCL of 303.5 ms in Control case, while at 142.7 ms for AF1 and 184 ms for AF2 cases.

Action potential (AP) and associated calcium ($[Ca^{2+}]_i$) transient for Control, AF1 and AF2 were computed using the Courtemanche et al. model by a series of supra-threshold stimuli with a pacing cycle length (PCL) of 1 s. The 10th AP and $[Ca^{2+}]_i$ transient were recorded for analysis. Changes in APD_{90} and peak $[Ca^{2+}]_i$ were noted. The cell models were incorporated into a reaction-diffusion parabolic partial differential equation (see for *e.g.* ref. [7]) to construct spatial models of electrical propagation. The eletrotonic diffusive coupling between cells simulating the gap junctional coupling was taken to be 0.03125 mm^2/ms to give a conduction velocity of 0.27 cm/s for a solitary wave under Control conditions. The 1D and 2D spatial models were constructed with a spatial resolution of 0.1 mm to give stable numerical solutions. The 3D anatomically detailed geometry of human female atria was obtained from [8]. It was taken to be electrically and spatially homogenous for the purposes of this study. Spatial resolution in the 3D anatomical model was 0.33 mm x 0.33 mm x 0.33 mm.

1D models were used to compute CV restitution (CVr) and temporal vulnerability window (VW). To compute CVr, a conditioning pulse stimulus was applied at one end of the strand, over a length of 0.3 mm with amplitude 2 nA and duration of 2 ms, after which a premature S2 stimulus was applied at the same location. The CV of resultant second propagation was computed as a function of the S1-S2 interval. To compute VW, the S2 was applied in the middle of the strand rather than at the conditioning stimulus end. The difference in the maximal and minimal values of the S1-S2 intervals that produced uni-directional propagation defined the VW. Re-entrant waves in 2D homogenous sheets of tissue (37 mm x 37 mm) were initiated using standard S1-S2 protocol [9]. and scroll wave re-entry in the 3D homogenous model was initiated in the largest contiguous surface of the right atrium using a cross-field protocol similar to that used in 2D idealized sheets of atrial tissue. Electrical activity of 5 s was simulated in each case and we registered APs at representative locations in the atria. Dominant frequency (DF) of these APs was computed using MATLAB functions and scripts developed in our laboratory.

Integration in time and space was carried out using an explicit Euler forward time step method while using central differences for spatial derivatives. The integration time step was taken to be 0.005 ms in the cell and 1D models. In the 3D simulations, a time step of 0.05 ms was seen to give solutions similar to the smaller time step of 0.005 ms as the space step was 0.33 mm, whilst satisfying stability criterions for spatio-temporal numerical integration. Simulations were carried out on (i) Sun-Fire 880 UltraSPARC 24 CPUs shared memory system, and (ii) Bull Itanium2 208 CPUs distributed memory system with a single rail Quadrics QsNetII interconnect. The 3D simulations were carried out using parallel OpenMP and MPI solvers developed in our laboratory. This allowed the simulations to be completed using both available resources. Due to run time limits on the multi-user parallel computers, check-pointing was implemented where the state of the model was stored to allow re-continuation of the simulation.

3. Results

AFER produced a dramatic APD_{90} abbreviation and reduction in $[Ca^{2+}]_i$ amplitude. APD_{90} was reduced by

65.3 % (108.5 ms) in AF1 and 52.8 % (147.6 ms) in AF2 cases, as compared to 313.0 ms in Control case, consistent with experimental observations [3, 4]. AFER hyperpolarized AP resting potential, which changed from -80.5 mV in the Control to -85.2 mV in AF1 and -83.8 mV in AF2 cases. $[Ca^{2+}]_i$ amplitude was significantly reduced from 0.61 μM in Control to 0.30 μM in AF1 and 0.31 μM in AF2 cases. Resting $[Ca^{2+}]_i$ was also reduced from 0.13 μM in control to 0.090 μM in AF1 and 0.094 μM in AF2. Simulated AP and $[Ca^{2+}]_i$ profiles are shown in Figure 1.

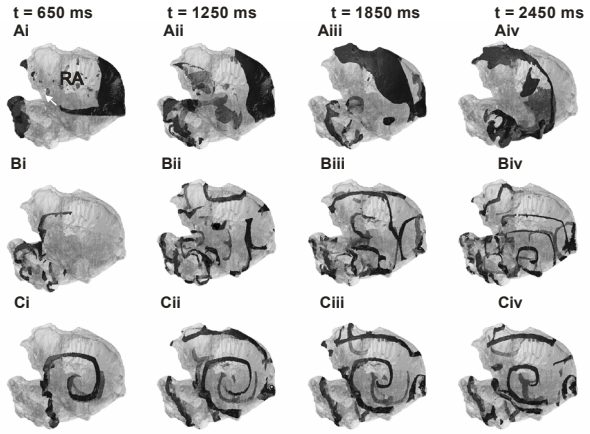

Figure 3. Scroll waves in the 3D model where transparent grey shows anatomy and solid black denotes excitation. Location of the scroll wave initiation site (right atrium, RA) and SVC are shown in Panel **Ai**. Panels **Ai-iv** show frames for Control simulation, **Bi-iv** for AF1, and **Ci-iv** for AF2. Frames were taken at times as shown at the top of each column. The scroll wave in Control meanders out of the RA at t ~ 2400 ms and its initial direction is shown in **Ai**. In AF1, the induced mother rotor breaks up into smaller persistent spiral wavelets. The scroll wave is stable with a small meander in the AF2 case.

CVr and VW were determined from the 1D models. Reduced excitability of atrial tissue due to AFER-induced hyperpolarization in cell AP is reflected in the reduced CV of a solitary wave from 0.27 cm/s in Control, to 0.25 cm/ms in AF1and 0.26 cm/ms in AF2. As shown in Figure 2 for CVr, atrial conduction is supported at much higher pacing rates under AF conditions as compared to control. When stimulus rate was 198 beats/min (S1-S2 interval < 303.5 ms) conduction failed in Control tissue. However with AFER, atrial tissue supported rate conduction up to 421 beats/min (S1-S2 interval ~ 142.7 ms) for AF1 and 325 beats/min (S1-S2 interval ~ 184 ms) under AF2 conditions. AF reduced VW from 15.4 ms in Control to 14.0 ms (10% reduction) in AF1 and 14.8 ms (4% reduction) in AF2 and cases.

In the 2D simulations, re-entry self terminated at t ~ 1800 ms in Control, but persisted for more than 6 s in the AF1 and AF2 cases. Frequency analysis of the AP waveforms gave us a DF of less than 4 Hz in Control, 11 Hz in AF1 and 8 Hz in AF2.

In the 3D simulations, scroll waves were induced on the largest contiguous surface of the RA. This offered the maximum possible substrate for the scroll waves to meander without anatomical interference. Figure 3 shows the evolution of scroll waves on the right atrial surface in the 3 cases. In the Control case, the scroll wave quickly meanders away from the point of initiation (~350 ms after initiation) and out of the tissue. In the AF1 case, the scroll wave was highly localized, but the mother rotor quickly degenerated into smaller wavelets. These wavelets continued to sustain erratic electrical activity throughout the homogenous model. After t = 2100 ms another mother rotor emerged. In the AF2 case, the scroll wave meandered in a very small region leading to a sustained scroll wave excitation driven by mother motor with indefinite lifespan (lifespan > 5 s of simulation duration). The scroll wave simulation is illustrated in Figure 3. The DF measured in the Control case was 3 Hz, but was about 6 Hz in AF1 and AF2 cases.

In the Control case when entrapped by an anatomical obstacle, the meandering scroll wave could also be stabilized with its filament pinned around the circumference of an anatomical obstacle. This is shown in Figure 4, where the scroll wave was entrapped to the opening hole of the SVC leading to persistent re-entry. In this case, the arm of this entrapped scroll wave continued to activate atrial tissue close to the SVC at a high rate. This gave rise to alternans type excitations, as shown by the AP profiles registered at various locations. Alternans were not observed in the AF1 and AF2 cases, however the AP profiles indicate excitation at a much higher rate in the AF cases as compared to Control.

We estimated the scalability of our 3D OpenMP and MPI solvers. The OpenMP solver had peak performance at 22 processors. The MPI solver scaled well and performance improved almost linearly till 32 CPUs. Typically, a single run simulating 5 s of activity in the anatomically detailed atrium took approximately 6 days of continuous running on a modest 12 processors.

4. Discussion and conclusions

Our simulation results have shown that AFER shortened atrial APD and reduced intra-atrial conduction velocity. These factors facilitated high rate atrial excitations and conduction as one would observe during AF. This suggested the pro-arrhythmic effects of AFER. In the 3D simulations, scroll waves underwent a large meander in the Control case. Such a strongly meandering scroll wave may self-terminate unless entrapped by

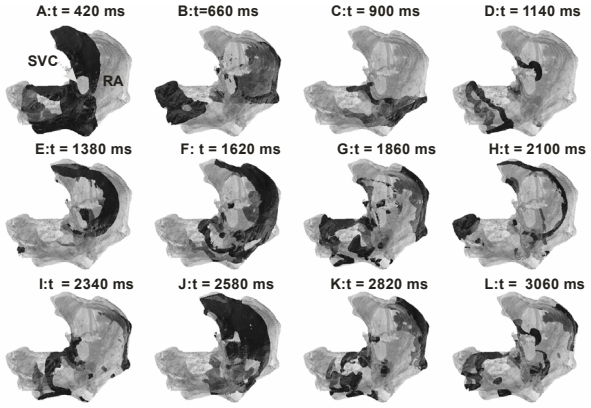

Figure 4. Frames from Control simulation showing entrapment of scroll wave by SVC (shown in **A**). After application of the re-entry inducing stimulus (**B**), the scroll wave quickly meanders away from the centre of the RA and was pinned to the SVC (**D**) opening.

anatomical obstacles formed by opening holes of valves. After being entrapped, the reentry sustained and acted as a mother motor to drive and pacing atrial excitation. AFER stabilized the scroll waves and reduced its meandering region. In this case, the scroll waves became more stationary and persistent, though it broke up leading to the formation of multiple wavelets (in the AF1 case). When this occurred, atria had erratic electrical excitation activity with much higher rates resembling the disordered and irregular electrical activity as shown by ECG in AF patients. Although APD shortening was greater in AF1 than AF2 case, stability of mother rotor in AF2 case was greater [8]. This can be directly related to the maximal slopes in APDr curves, where slope AF1 is greater than slope in AF2. The relationship between APDr and propensity towards fibrillation has been previously established in clinical and computational studies [10, 11]. We concluded that AFER is pro-arrhythmic, helps to perpetuate and sustain re-entrant excitation in atria. This study provides evidence in support of the hypothesis of AF begetting AF [12].

Acknowledgements

This work was supported by the British Heart Foundation , UK (PG/03/140).

References

[1] Lip GY, Tello-Montoliu H, Management of Atrial Fibrillation. Heart. 2006; 92: 1177-1182.

[2] McDonald AJ, Pelletier AJ, Ellinor PT, Camarqojr CA. Increasing US Emergency Department Visit Rates and Subsequent Hospital Admissions for Atrial Fibrillation from 1993 to 2004. Amm. Emerg Med. 2007; Epub Ahead of Print.

[3] Bosch RF, Zeng X, Grammer JB, Popovic K, Mewis C, Kühlklamp V. Ionic mechanisms of electrical remodelling human atrial fibrillation. Cardiovasc. Res. 1999; 44: 121-131.

[4] Workman A, Kane KJ, Rankin AC. The contribution of ionic currents to changes in refractoriness of human atrial myocytes associated with chronic atrial fibrillation. Cardiovasc. Res. 2001; 52: 226 – 235.

[5] Courtemanche M, Ramirez RJ, Nattel S. Ionic mechanisms underlying human atrial action potentials: insights from a mathematical model. Am. J. Physiol. 1998; 275: H301 - H321.

[6] Zhang H, Garratt CJ, Zhu J, Holden AV. Role of upregulation of IK1 in action potential shortening associated with atrial fibrillation in humans. Cardiovasc. Res. 2005; 66(3): 493 – 502.

[7] Zhang H, Kharche S, Holden AV, Hancox JC. Repolarisation and vulnerability to re-entry in the human heart with short QT syndrome arising from KCNQ1 mutation — A simulation study. Prog. Biophys. Mol. Biol. (In press).

[8] Seemann G, Höper C, Sachse FB, Dössel O., Holden AV, Zhang H. Heterogeneous three-dimensional anatomical and electrophysiological model of human atria. Phil. Trans. Roy. Soc. A. 2006; 364(1843): 1465–1481.

[9] Kharche S, Seemann G, Leng J, Holden AV, Garratt CJ, Zhang H. Scroll waves in 3D Virtual Atrium: A Computational Study. In F B Sachse and G Seemann (Eds). LNCS. 2007; 4466: 129-138.

[10] Byung-Soo K, Young-Hoon K, Gyo-Seung H, Hui-Nam P, Sang Chil L., Wan Joo S., Dong Joo O., Young Moo R. Action Potential Duration Restitution Kinetics in Human Atrial Fibrillation. J. Am. Col. Cardiol. 2002; 39(8): 1329 - 1336.

[11] Xie F, Qu Z, Garfinkel A, Weiss J. Electrical refractory period restitution and spiral wave reentry in simulated cardiac tissue. Am J Physiol Heart Circ Physiol. 2002; 283: 448 - 460.

[12] Wijffels M, Kirchof CJHJ, Dorland R, Allessie MA. Atrial Fibrillation Begets Atrial Fibrillation: A Study in Awake Chronically Instrumented Goats. Circulation. 1995; 92: 1954 – 1968.

Address for correspondence:
Name: Dr. Sanjay Kharche
Full postal address: School of Physics and Astronomy, Schuster Building, University of Manchester, Manchester, M13 9PL, UK.
E-mail address: Sanjay.Kharche@manchester.ac.uk